International Journal of Science and Research (IJSR)
ISSN: 2319-7064
Impact Factor 2024: 7.101

A Study of Chlorophyll Variation under the Influence of the Western Boundary Current System of Atlantic and Pacific Ocean Sectors of the Southern Ocean

Dr. Nibedita Behera

Department of Marine Sciences, Berhampur University, Bhanjabihar 760007, Odisha, India
Corresponding Author Email: *nbeheraoc91[at]gmail.com*

Abstract: ***The south western part of the Atlantic and Pacific sector plays a unique role in terms of ocean currents and variation in Chl-a. The Atlantic part of the study region contains the confluence region of two current system named Brazil current and Malvinas current. And the western part of the Pacific region is one of the thrive place for coral. This study represents the connection of the Chl-a variation along with the seasonal and inters annual variation of the respective current systems. The Chl-a in the Brazil Malvinas Confluence area is boosted by the nutrient-rich coastal water of the Brazil Current. During the summer, Chl-a reached a peak of 1.6 mg m^{-3} (log10 scale) and then fell to 2.5 mg m^{-3} (log10 scale) during the winter in this region. In La Niña, the dominance of the nutrient rich Malvinas current favors the enhancement of Chl, whereas wind plays an important role in mixing and enhancement of Chl-a in the positive phase of SAM. The East Australian Current (EAC) of the Pacific region is strongest in the summer and gradually weakens in the winter. More dominant EAC means the lesser intrusion of Tasmania Sea water in this region. Frontal eddies resulted from the mixing of these two water masses, which is one of the reasons for Chl-a in the offshore area. In La Niña, the strength of the EAC decreased and hence the influence of nutrient rich polar water increases, which leads to a higher Chl-a of 2.5 mg m^{-3} (in log10 scale) in the shelf region and 0.8 mg m^{-3} (in log10 scale).***

Keywords: ocean currents, chlorophyll variation, Brazil Malvinas Confluence, East Australian Current, seasonal changes

1. Introduction

In the Southern Atlantic Ocean, an interaction occurs between the southward flowing Western Boundary Current (WBC) of subtropical gyre named Brazil Current (BC) with a northward flowing Malvinas Current (MC), which is a northward extension of Antarctic Circumpolar Current (ACC) (Fig. 1a). At 38°S, the southward-moving coastal BC turns southeast and meanders back towards the north (Goni and Wainer, 2001). Due to the topographic impact, the ACC's sub Antarctic front (SAF) shifted northward instead of eastward. Between the North Scotia Ridge and the Malvinas Plateau, this deviated SAF flows northward and becomes the Malvinas Current, which runs along Argentina's coast (Artana et al., 2016). The Brazil Malvinas Confluence Zone is formed when these two currents meet at 38°S. (Gordon 1989). The confluence zone's location varies not only seasonally but also interannually. Variations in transport in the BC or MC may be one of the reasons for changes in the confluence region. The local wind field also has an effect on the BMC confluence region's variation (Garzoli and Giulivi, 1994). However, the origin of this seasonal variation is unknown (Jullion et al., 2010). Similarly, the EAC is the southern Pacific subtropical gyre's WBC that primarily governs the biological properties of continental shelf water off East Australia (Nilsson and Cresswell, 1981; Hassler et al., 2011) (Fig. 1b). Seasonal variations in EAC are largely responsible for the water properties on the shelf (Ridgway and Godfrey, 1997). When EAC flows very close to the shore, it displaces the coastal water, resulting in upwelling events and the creation of eddies (Oke and Middleton, 2000). Both upwelling and eddies always provide optimal conditions for phytoplankton to develop to its maximum potential, making the coastal regions productive with higher Chl. In terms of these oceanic processes together with the seasonality of Chl-a variation in the EAC zone, can lead to significant variations in the seasonality of Chl-a in both domains. The seasonal variations in Chl, as well as the relative impact of wind stress and eddies on the Chl-a variability, are crucial to understand.

Subtropical water is oligotrophic in nature, whereas polar water is rich in nutrients. The strength of polar water currents into the subtropics varies not only on the seasonal scale but also on the interannual time scale by the influence of ENSO and SAM events. This variation in polar water intrusion is one of the factors of the regional variation of Chl-a in the subtropics regions. Thus, this chapter is particularly focused on the seasonality and inter-annual variation of subtropical Chl-a with respect to the variation in the intrusion of polar water and associated physical processes like frontal eddies and coastal upwelling.

The biological productivity associated with the cold current system i.e. Eastern Boundary Current (EBC) is well documented (Carr, 2021; Correa-Ramirez et al., 2012; Carr and Kearns, 2003; Thomas et al., 2004). The thermal front is significant in the western southern part of the Tropical Ocean and Southern Ocean.

2. Data and Methodology

The details of datasets used for this study and formulation used for the investigation of seasonal and inter-annual variations of Chl concentration are discussed in this section.

Discrete and sparse availability of in situ data in this region makes it challenging to detect the spatial Chl concentration variability in this region. However, remotely sensed satellite observations and model simulated reanalysis datasets are the potential datasets to investigate the oceanic processes in this region.

2.1. Data Used

2.1.1. Satellite data

The monthly Chl-a, sea surface temperature (SST) and Photo synthetically available radiation (PAR) are taken from the Moderate Resolution Imaging Spectroradiometer (MODIS) on board satellite Aqua, level 3 with a spatial resolution of 4 km x 4 km during the period July 2002 to December 2010. These are obtained from the Ocean Color group of Goddard Space Flight Center (GSFC), National Aeronautics and Space Administration (NASA) (source: http://oceandata.sci.gsfc.nasa.gov). The Chl-a data from MODIS-Aqua is well validated in earlier studies (Tilstone et al. 2013).

The monthly Sea Surface Height Anomaly (SSHA) data for the same time period is obtained from the AVISO (Archiving, Validation, and Interpretation of Satellite Oceanographic data). It is a merged product of TOPEX/Poseidon and ERS satellites, with a spatial resolution of 25 km (source: https://www.aviso.soest.hawaii.edu). The SSHA is an adequate parameter to represent the mesoscale cyclonic and anticyclonic features in a region associated with the path of a current system (Ducet et al. 2000; Richardson et al. 2003; Rouault et al. 2010; Huang and Feng 2015). Subsurface information is required for understanding the subsurface dynamics and possible mechanisms involved. Hence, the model reanalysis datasets are used in this study as explained in the next section.

2.1.2. Climate indices

This paper also examined the interannual variability of Chl-a according to different phases of ENSO and SAM. The Station based Marshall SAM index is archived from https://climatedataguide.ucar.edu/climate-data/marshall-southern-annular-mode-sam-index-station-based (Marshall, G.J., 2003). This index is calculated from the pressure difference between the two-fixed latitude of 40°S and 65°S. Three month running mean of Oceanic Niño index (source: https://climatedataguide.ucar.edu/climate-data/Niño-sst-indices-Niño-12-3-34-4-oni-and-tni) is used in this study (Trenberth and Stepaniak 2001). Positive Oceanic Niño index refers to El Niño whereas negative value indicates the La Niña phase.

2.2. Methodology

2.2.1. Selection of regions

The standard deviation of monthly Chl-a from 2003 to 2017 is used to obtain the spatial variability of chlorophyll-a in the region (Fig. 2). The variability in coastal Chl-a in this region is quite high at 10 mg m^{-3}. Higher Chl-a along the coast is also notable for its proximity to the continental slope region, which has bathymetry ranging from 200 to 1000 m. Near the mouth of the Rio de la Plata, the coastal variation of the BMC showed a higher Chl-a variation of 10 mg m^{-3} (box (a)) than the other study region (Fig. 2). The Rio de la Plata's mouth is well known as the world's most dynamic and variable estuarine structure (Telesca et al., 2018).

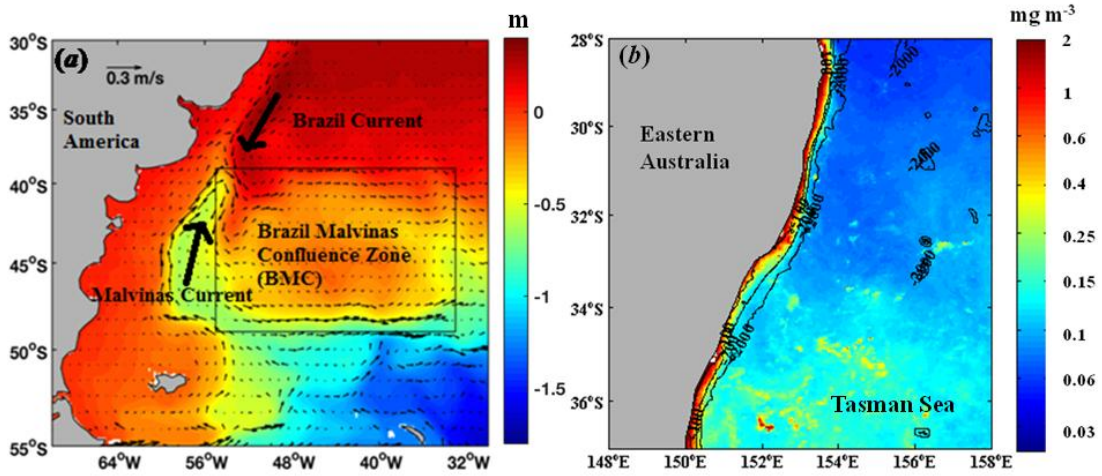

Figure 1: (a) Study region in the Atlantic Ocean: averaged geostrophic currents derived from sea surface height anomaly from 2003-2017. (b) Study region in the Pacific Ocean: the spatial map of the standard deviation of chlorophyll-a concentration (shaded in mg m^{-3} in log10 scale). The black contours show the bathymetry from ETOPO2. 'BMC' stands for Brazil Malvinas Confluence Zone

2.2.2. Geostrophic Velocity

Physical processes, which influence upwelling, like cross-frontal mixing, geostrophic current etc. can control the Chlorophyll distribution in our study region, have been considered for the further analysis (Anilkumar et al. 2015, George et al. 2018). The mesoscale eddies play an important role in bringing up nutrients to the surface (Frenger 2013). Hence, the study of variations in eddy positions in conjunction with ARC is crucial. In this study, the geostrophic currents derived from SSHA have been used for the aforementioned domain.

Geostrophic currents are generally derived from the SSHA (η). The components u and v of the geostrophic velocity are defined as follows

$$u_{geo} = -\left(\frac{g}{f}\right).\frac{\delta\eta}{\delta y}$$

$$v_{geo} = \left(\frac{g}{f}\right).\frac{\delta\eta}{\delta x}$$

Where, u represents the zonal component, v the Meridional components.

The tools used for finding the seasonal and interannual variations of different parameters and the method used for evaluating the correlation between them are discussed in the following section. For seasonal analysis four seasons are considered; a) Austral Spring (September – November) b) Summer (December – February) c) Autumn (March –May) d) Winter (June – August).

3. Results and Discussion

3.1. Chlorophyll variability in the Atlantic Ocean sector of the Southern Ocean

Sea surface temperature (SST) always plays an important role in the variation of Chl-a concentration in the ocean (Ji et al., 2018; Kavak and Karadogan, 2012). The study region of BMC is a mixture of both cold fresh polar water and warm saline subtropical water. The complexity of this region is that the seasonal and inter-annual variation of both currents may affect the variation of Chl-a due to changes in water properties. Investigation of the spatial variability of both SST and Chl-a in this region is crucial to understand the relation between the two parameters in the study region.

3.1.1. Spatial variation of Chlorophyll-a

The standard deviation of monthly Chl-a from 2003 to 2017 is used to obtain the spatial variability of chl-a in the region (Fig. 2). The variability in coastal Chl-a in this region is quite high at 10 mg m^{-3}. Higher Chl-a along the coast is also notable for its proximity to the continental slope region, which has bathymetry ranging from 200 to 1000 m. Near the mouth of the Rio de la Plata, the coastal variation of the BMC showed a higher Chl-a variation of 10 mg m^{-3} (box (a)) than the other study region (Fig. 2). The Rio de la Plata's mouth is well known as the world's most dynamic and variable estuarine structure (Telesca et al., 2018).

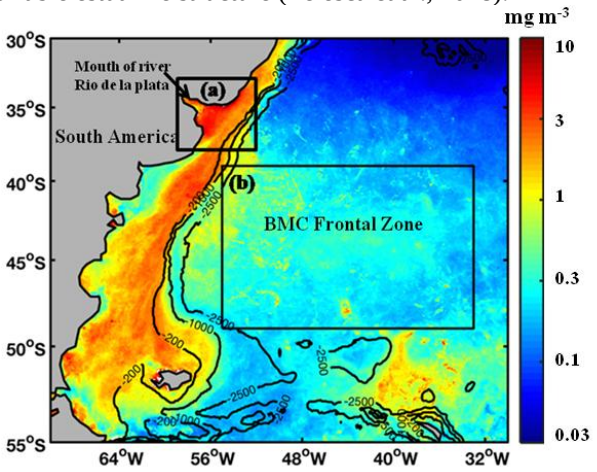

Figure 2: Standard deviation of Chl-a (log10 scale) from January 2003 to December 2017. Box (a) indicates the mouth of the river Rio de la Plata, and box (b) represents the open ocean (Brazil Malvinas Confluence Zone) BMC zone

The high variability of Chl-a in region 'a' (38.5°S to 33.5°S and 53°E to 58°E) is considered to be the consequence of the variation in the coastal processes, which include the sediment influx by the river Plata, the resuspension of sediment and the residence time of nutrient (Martinez and Ortega, 2015). The wave effect and the near-shore circulation pattern influence phytoplankton production in this region (Campos et al., 1999; Simionato et al., 2004, 2005). It was recognized that anthropogenic nutrient discharge, as well as climate change, could impact the nutrients in the river Plata's mouth region over time (Acha et al., 2008). The rest of the shelf (except for box (a)) is mainly influenced by nutrient-rich polar water, which does explain the Chl-a variability in the region. The open ocean region of BMC is depicted in box 'a', which is far from the river Plata 'b'. The confluence of the Brazil and Malvinas current, on the other hand, has the capacity to transport nutrients discharged from the river in this area (Fig. 2). This may be one of the reasons for the Chl-a variation in the open ocean (box 'b'). The variation in the concentration of Chl-a in the box (b) is in between the sub-tropic (less Chl-a, 0.3 mg m^{-3} in log10 scale) and in the polar region (1.25 mg m^{-3} in log scale). The south-eastern part of the study region, that is below the box (b) showed a higher variation in Chl-a concentration of (1.25 mg m^{-3}, possibly due to shallow bathymetry. Eddies are formed when the current interacts with the bathymetry, and they are one of the factors contributing to the rise in Chl-a. In addition, phytoplankton can also thrive due to the shallow bathymetry. The seasonal and interannual variations of Chl-a in the BMC are discussed in detail in the later sections.

3.2 Spatial Variation of Sea Surface Temperature

The fusion of warm saline subtropical water with cold fresh polar water occurs in the study region. The cold polar currents dominate the coastal shelf and open ocean BMC regions, as shown in Fig. 3. And as a result of the fusion, a large SST gradient is observed. In both the coastal and open ocean areas, SST varies from 7 to 16 ˚C. The intrusion of the cold polar water follows the isobaths of 200 m to 2500 m. The variation of SST in the range 24˚C - 18˚C is observed from 30˚S to 40˚S which dominated the subtropical water. From 50˚S to 55˚S the dominance of the polar water is observed, as the variation of SST is between 1˚C - 7˚C.

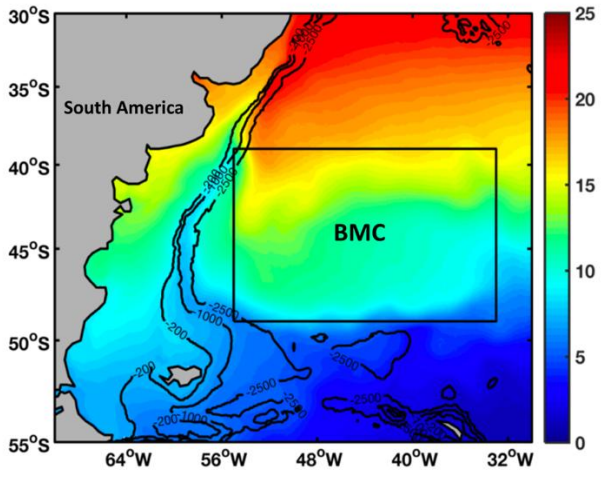

Figure 3: Mean SST from January 2003 to December 2017

3.3. Seasonal Variability of Chlorophyll-a and other Influencing Factors

In this section the seasonal variability of the SST and PAR, and their relations with the Chl-a variability are discussed. It also analyzed the influence of the river water into the BMC region.

3.3.1. Seasonal Variability of Chlorophyll-a

One of the peculiarities of Chl-a variability in the region is that the Chl-a concentration is always high in the mouth of the river Plata irrespective of the season (Fig. 4). The confluences of Brazil and Malvinas currents, and the different water mass properties show that most of the river driven nutrients are contained within the river mouth of Plata. Seasonal variation was particularly noticeable along the southern region of the coastal area (Fig. 4). During the spring season, the maximum Chl-a concentration was 6.3 mg/m^3 along the southern coast from 38 to 54 ˚S.

There was a lower concentration of Chl-a along the east coast, from 38˚S S to 42˚S, compared to the other coastal area. A distinct concentration of Chl-a was observed along the course of the Malvinas current (refer to Fig. 1). This is more general in the autumn and winter seasons, as seen in figures 4 (c) and (d). Seasonality is also observed in the Brazil-Malvinas confluence area (box in Fig. 4). The seasonal Chl-a concentrations observed in the study region ranged as follows: summer season (2 – 1 mg m^{-3}) > spring (1.4 – 10 mg m^{-3}) > autumn (0.6 – 2.5 mg m^{-3}) > winter (0.39 – 4 mg m^{-3}). Seasonality in Chl-a in the studied area could be caused by seasonality in temperature, PAR, current intensity and zonal and vertical distribution, nutrient availability, or other oceanic processes such as eddies. Each of the parameters is analyzed separately.

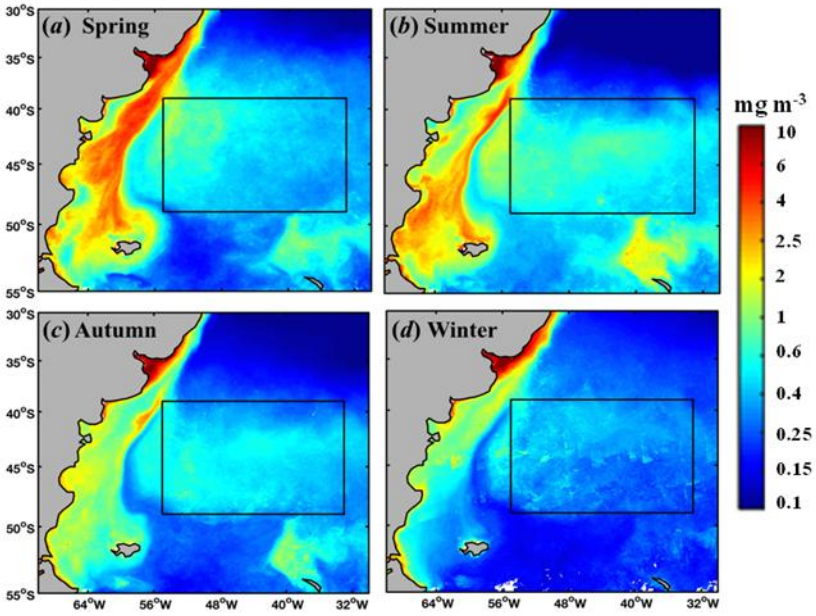

Figure 4: Seasonal averaged Chl-a (in log10 scale) during (a) Summer (b) Autumn (c) Winter (d) Spring. 'BMC' denotes the Brazil Malvinas Confluence Zone'.

3.3.2. Seasonal Variation of Sea Surface Temperature

The seasonality of SST is not only dependent on solar radiation but on the properties of the water mass as well. The place of origin of water mass is also one of the defining factors for regional or distant water mass's SST characterization. Cold SST followed the path of the Malvinas current and moved northward along the continental shelf region (Fig. 5). During the winter and spring seasons, cooler SST was more prominent in the continental shelf region, ranging between 2 - 4˚C along the Malvinas current. SST varied between 8 – 14 ˚C during the summer and autumn seasons. During summer and autumn, SST varied between 23 - 25˚C along the Brazil current (Fig. 5b and c).

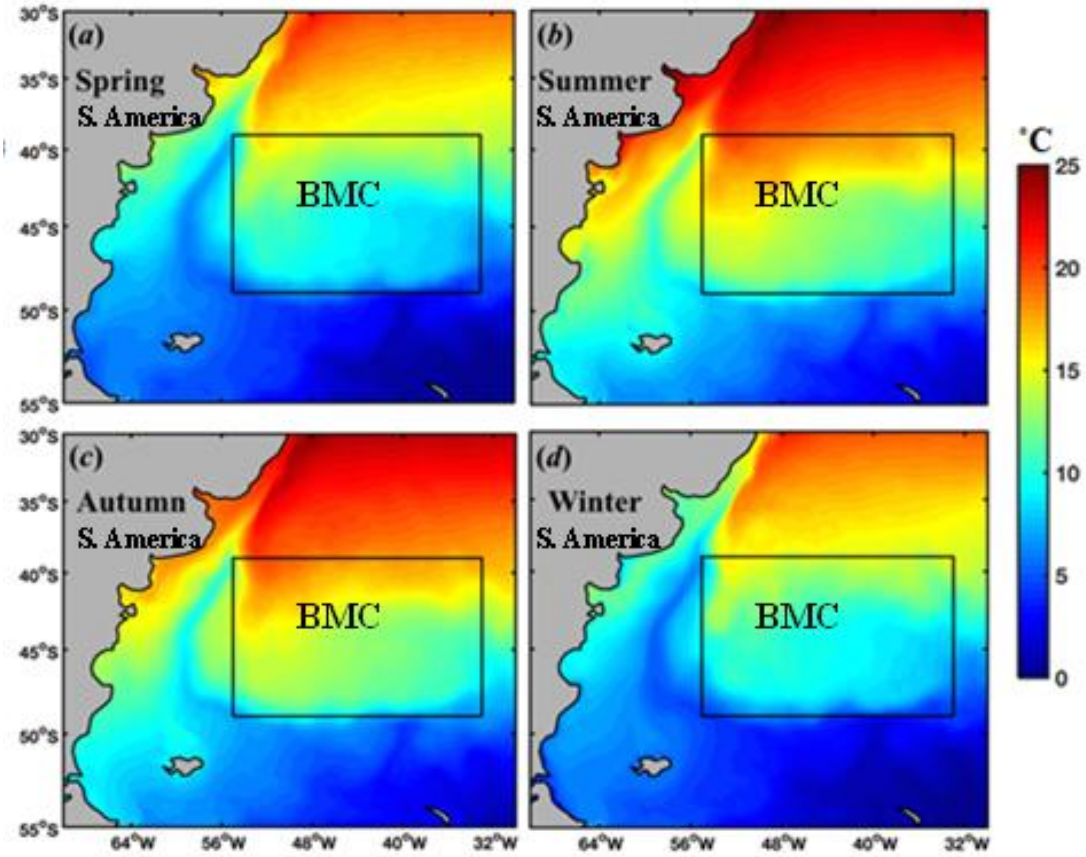

Figure 5: Seasonal Variation of SST during (a) Summer (b) Autumn (c) Winter (d) Spring. 'BMC' denotes the Brazil Malvinas Confluence Zone'

During the spring and winter, the SST dropped to 15-19°C (Fig. 5a and d) in the BMC. The subtropical higher water mass dominates the northern part of the BMC open ocean area (rectangular box in Fig. 5), with higher SST in the range of 19-20 °C in summer and autumn and 15-17 °C in spring and winter.

Though the southern part of the box is dominated by the cold polar water, a clear seasonal variation of SST could be detected not only in its temperature but also in the northward extent of the polar water. During the winter and spring, the polar water extends further north. The SST ranges between 1-3 ˚C in the open ocean and 5-7 ˚C in the coastal area. The influence of the polar water in the coastal region is decreased from the winter, spring, autumn and summer. The higher Chl-a is detected in the lower SST region (Fig. 5). The possible reason for higher Chl-a is owing to the frontal nutrient enrichment in this region (Brandini et al., 2000), which is seen in the spring season. The limitation of sunlight during winter is one of the reasons for the lesser Chl-a in this region (Brandini et al., 2000).

3.3.3. Seasonal Variation of Photosynthetically Active Radiation

A clear seasonal variability of PAR was observed in southwester Atlantic Ocean. Irrespective of the season, the coastal region from 30˚S to 45˚S showed a higher PAR than that of the rest of the study area. PAR is observed to be highest during the summer season, followed by spring, autumn, and winter (Fig. 6). During spring, the coastal PAR ranges from 58 to 50 E m^{-2} d^{-1}. PAR values vary between 50 to 35 E m^{-2} d^{-1}, mostly south of 48˚S.

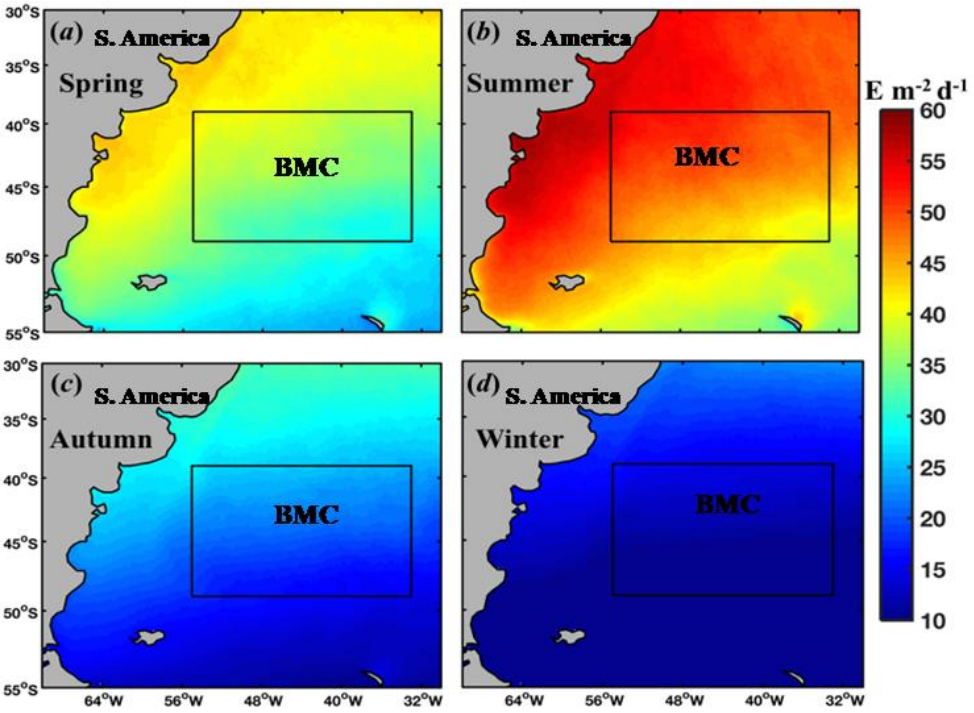

Figure 6: Seasonal averaged Photosynthetically Active Radiation (PAR) during austral (a) Summer (b) Autumn (c) Winter (d) Spring. 'BMC' denotes the Brazil Malvinas Confluence Zone'.

3.3.4. Seasonal variation of Geostrophic current

The warm subtropical water is being carried southward by the Malvinas current (Fig. 5). The study of Casey and Adamec (2002) concluded that high (low) SSHA is one of the indications of the current carrying warm (cold) water. Due to the subtropical gyre in the south Atlantic the SSHA in positive in the northern part of the study domain (Fig. 7). In the contrast, the region associated with polar cold water has negative SSHA. The confluence of Brazil and Malvinas current occurred at ~38˚S (Fig. 7) (Telesca et al., 2018). Higher SSHA of 1m indicated the dominance of the Brazil current during the austral summer and autumn seasons (Fig. 7b and c).

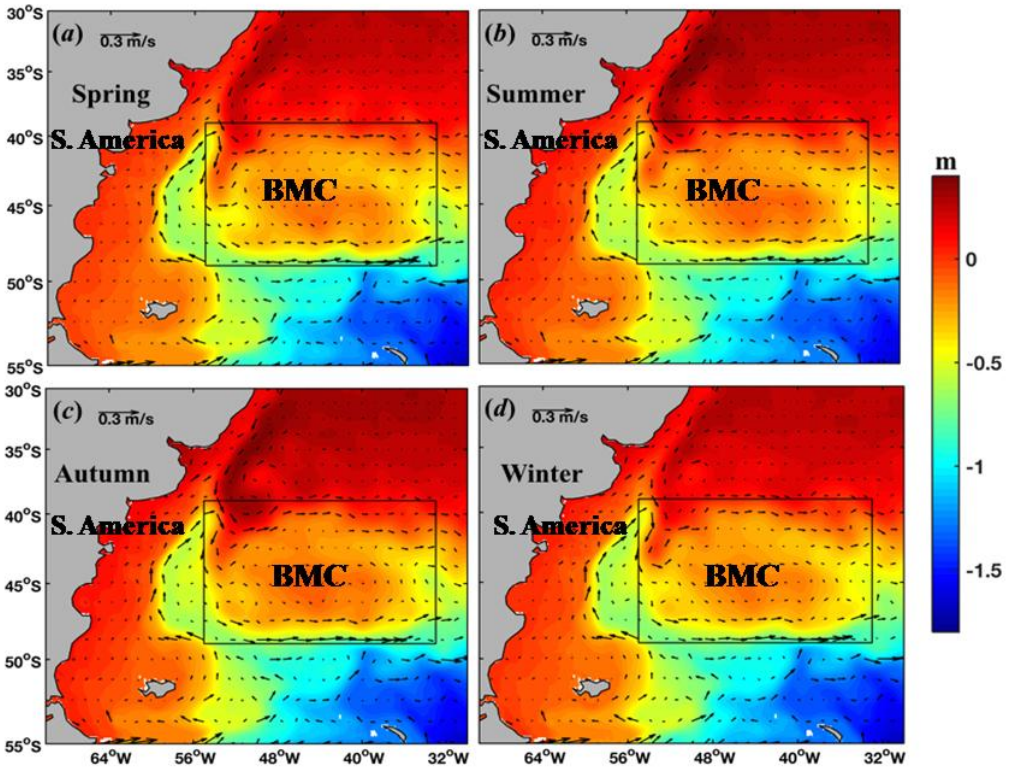

Figure 7: Geostrophic Current during austral (a) Summer (b) Autumn (c) Winter (d) Spring

Similarly, the SSHA of 0-0.5 m offshore of the confluence zone indicates that summer and autumn are dominated by subtropical water. Regardless of the austral seasons, there is no discernible shift in the strength of the Malvinas current. This suggests that the Brazil current is primarily responsible for variations in the open ocean BMC region's water mass.

3.4 Influence of river Rio de la Plata on Chlorophyll Concentration

The Rio de la Plata is the world's fifth largest estuary basin (Aubriot et al., 2020). In order to investigate the effect of the river Rio de la Plata over the open ocean BMC area, we used the Chl-a concentration in the river mouth instead of river inflow to the ocean. Box 'a' in figure 2 is considered for the region of river mouth of river Rio de la Plata. The open ocean BMC area is shown in Fig. 2 as box 'b'. The area average Chl-a concentration of both the boxes indicated that the higher concentration of Chl-a in the open ocean BMC region is followed by the higher Chl-a of the river mouth Chl (Fig. 8).

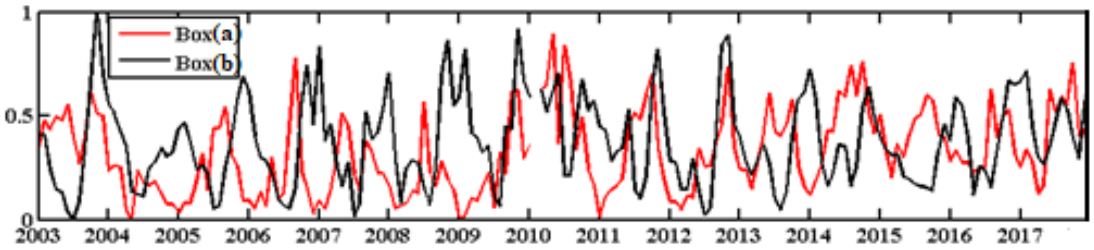

Figure 8: Normalized Chl-a of Box A (River Rio de la Plata) and Box B (open ocean BMC)

In 2004, the BMC area had a Chl-a concentration of 1 mg m^{-3} (normalized), while the river mouth had a Chl-a concentration of just 0.6 mg m^{-3}. A similar pattern can be seen in 2008 when the Chl-a concentration is 0.8 mg m^{-3}, but the river mouth Chl-a is 0.5 mg m^{-3}, and there is a 2–3 month lag between the peak Chl-a of the box 'a' and box 'b'. Inter-annual periodicities are found, which may be linked to changes in the Rio de la Plata's discharge caused by the El Niño phenomenon (Telesca et al., 2018). Behera et al. (2020a) found that 2008 is a year of the La-Nina, which is one of the reasons for the Agulhas current's weakening. This might happen in this location as well. A decrease in the strength of the BC during La Nina could be one of the factors for less advection of nutrients by the BC to the BMC region. The Malvinas' dominance could be linked to the increased Chl-a in the BMC in 2008.

3.5 Chlorophyll variability in BMC during ENSO and SAM

The concentration of Chl-a of BMC is above normal Chl-a of 0.2 mg m^{-3} in 2003, 2010, 2011 and 2017. The year 2003 is as a normal year for both SAM (< ±1) and ENSO (< ±1). The indices do not give any larger variation in this year (Fig. 9a and b).

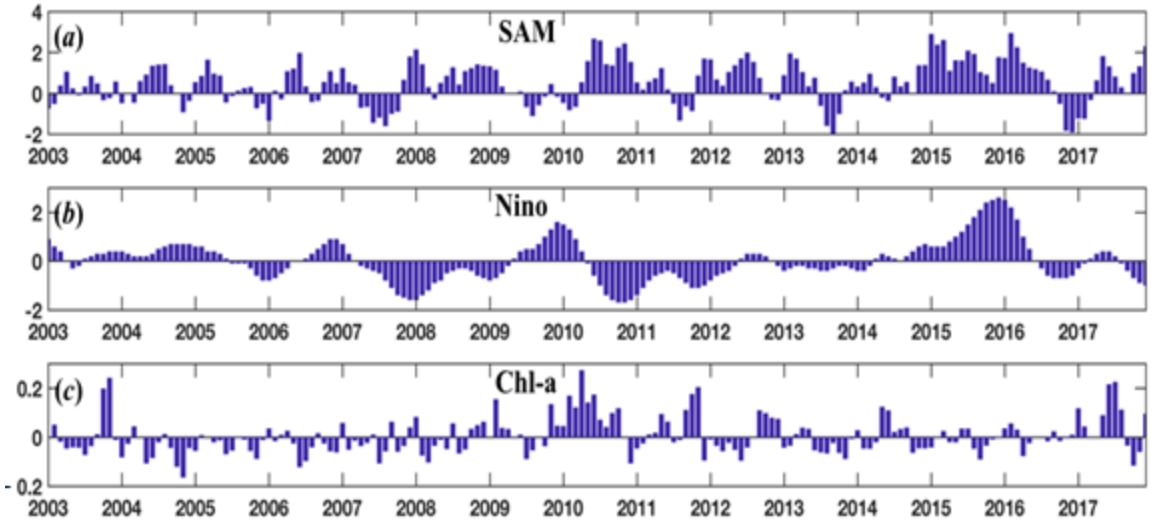

Figure 9: Time series of (a) SAM index (b) Nino index and (c) Chl-a (mg m^{-3}) monthly anomaly

The year 2010 is La Niña year (Nino index is less than -0.1 (-1.8)) and a positive SAM year (SAM index > 1). (Fig. 9a and b). 2010 is a La Nina year (Nino index less than 0.1 (-1.8)) and a year with a positive SAM index (SAM index > 1). Both positive and negative SAM indices were found in 2011, with a negative index of -1. In 2017, a positive SAM year with a SAM index greater than one was observed with a normal ENSO year. According to the results of the preceding analysis, the Chl-a of the BMC region increases during La Nina or positive SAM years.

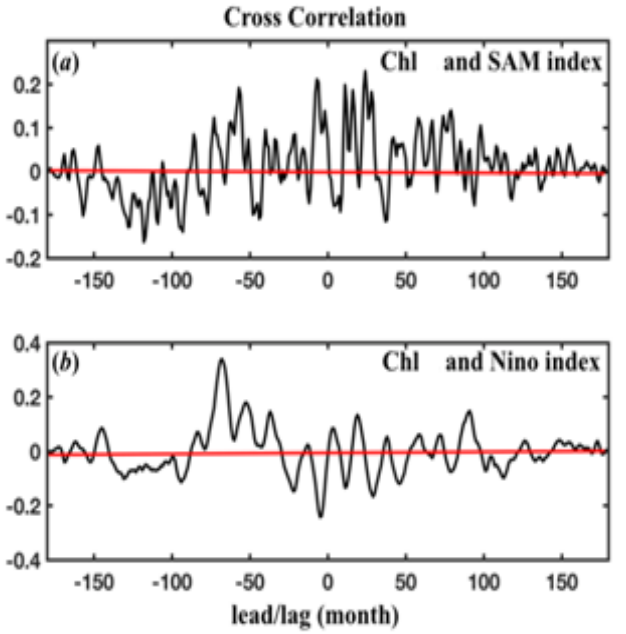

Figure 10: Cross correlation between Chl-a anomalies with (a) SAM and (b) Nino index

A cross correlation between Chl-a concentration and the SAM and Nino index was carried out to understand the influence of SAM and Nino index on Chl-a variability and the result is presented in Fig. 5.10. With a 6-month lag, a negative correlation is noted between the Nino index and Chl. ENSO's cycle lasts between 2 and 7 years (McPhaden et al., 2006). La Nina may also be one of the causes of greater Chl-a in the BMC region. With a one-year lead, Chl-a exhibited a positive relationship (+0.2) with the SAM index. In intra-seasonal (Hudson et al., 2011; Marshall et al., 2012) and seasonal (Hendon et al., 2013; Lim et al., 2013) time scales, SAM is now recognized as a source of predictability of Chl-a variability.

3.6. Chlorophyll variability in the Pacific Ocean sector of the Southern Ocean

3.6.1. Variability of Chl-a with SST

The southern portion of the retroflection of the East Australian Current (EAC) below 32 ˚S. A higher variability of 6.3 to 2 mg m^{-3} (in log_{10} scale) is noted on the south of EAC (Fig. 11). In the northern part, the EAC is more confined to the coast and the strongest down to the continental slope area.

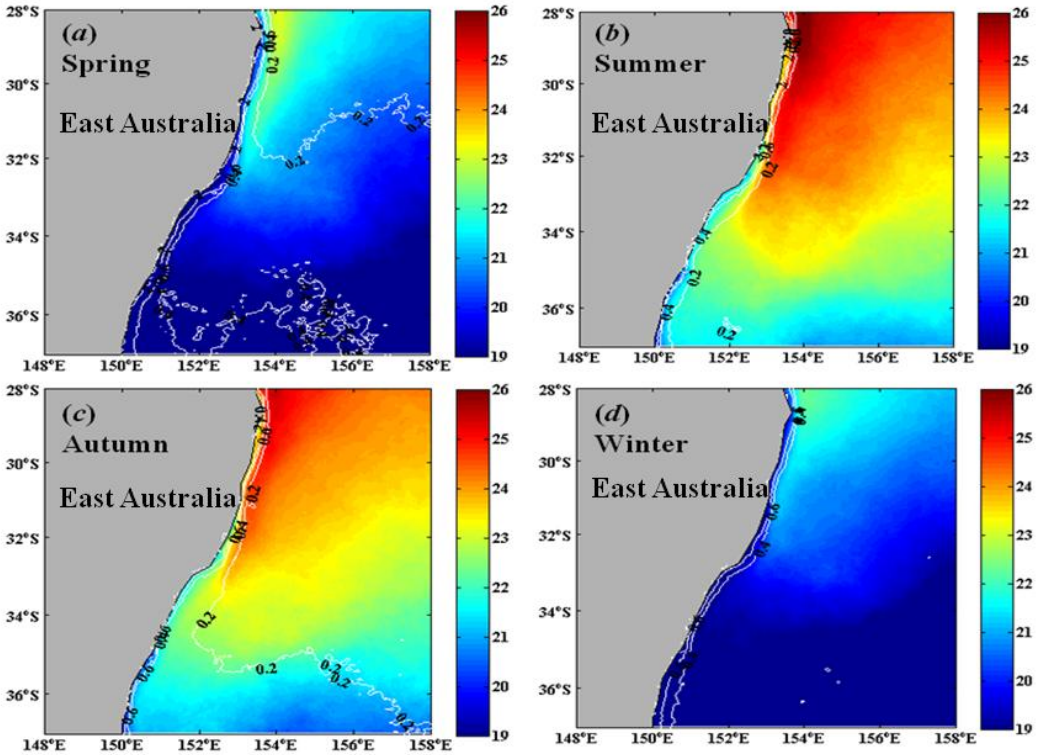

Figure 11: Seasonal climatological (2003-2017) variation of SST (shaded in ℃) for a) Austral Spring (September – November) b) Summer (December – February) c) Autumn (March-May) d) Winter (June – August) with white contours of Chl-a in mg m^{-3}.

This enhances the coastal process, and coastal upwelling events are mostly contained within the continental slope region. The open ocean part is devoid of these processes and showed less variability. On proceeding to the south, the EAC was reflected eastward at 32 °S, resulting in the mixing of warm subtropical water with polar Tasmania Sea water, which resulted in a frontogenesis process, a source for Chl-a enhancement in this region.

3.6.2. Seasonal variability of Chlorophyll and Currents

SST may be used as a proxy for EAC to study its seasonal variation since EAC primarily transports warm subtropical water. Fig. 12 presents the seasonal climatological SST variation in the region. The existence of the EAC can be easily seen from the warm signature of SST in Fig. 12. The strength of EAC is greater during the summer and spreads away from the coast.

EAC is more dominant offshore during summer. Chl-a is restricted to the shelf waters during this season. Since the EAC prevents shelf water from moving beyond the shelf and current-driven coastal upwelling events are limited to the shelf area, the shelf region has higher Chl-a concentrations (Roughan and Middleton, 2002; Roughan et al., 2003; Roughan and Middleton, 2004). From summer to winter, the intensity of EAC gradually decreases. During the autumn season, the EAC's intensity decreases significantly, and the EAC's influence narrows down to the coast. The Tasmanian Sea water moves northward, and Chl-a can be found to the south of the EAC retroflection. In the following sections, the seasonal dynamics are examined and explored further. With the approaching winter, the EAC is no longer observable, and cold water dominates the area. The offshore field had no Chl, but the shelf had a Chl-a of 0.4 mg m^{-3} , which is much lower than the summer season Chl-a of 2 mg m^{-3} (Fig. 12) Interestingly, the north of EAC's retroflection (north of 32˚S) had a Chl-a concentration of 0.2 mg m^{-3} during the spring season. The reason for a more northerly abundance of Chl-a is explored hereafter.

3.6.3. Seasonal Variability of Geostrophic Currents and Eddies

The geostrophic current vectors along with Chl-a contours for different seasons in the study region in the EAC region are shown in Fig. 12. The coastal upwelling is clearly evident in Fig. 13b throughout the austral summer in the form of a negative sea height anomaly. Further, an anticyclonic eddy was observed just south of the retroflection that is below 32˚S, leading to reduction of Chl-a value to 0.1 mg m^{-3}. The opposite is seen in winter (Fig. 12d). Coastal downwelling occurs during the winter season, resulting in reduced nutrient availability and, as a result, lower Chl-a levels in the coastal areas.

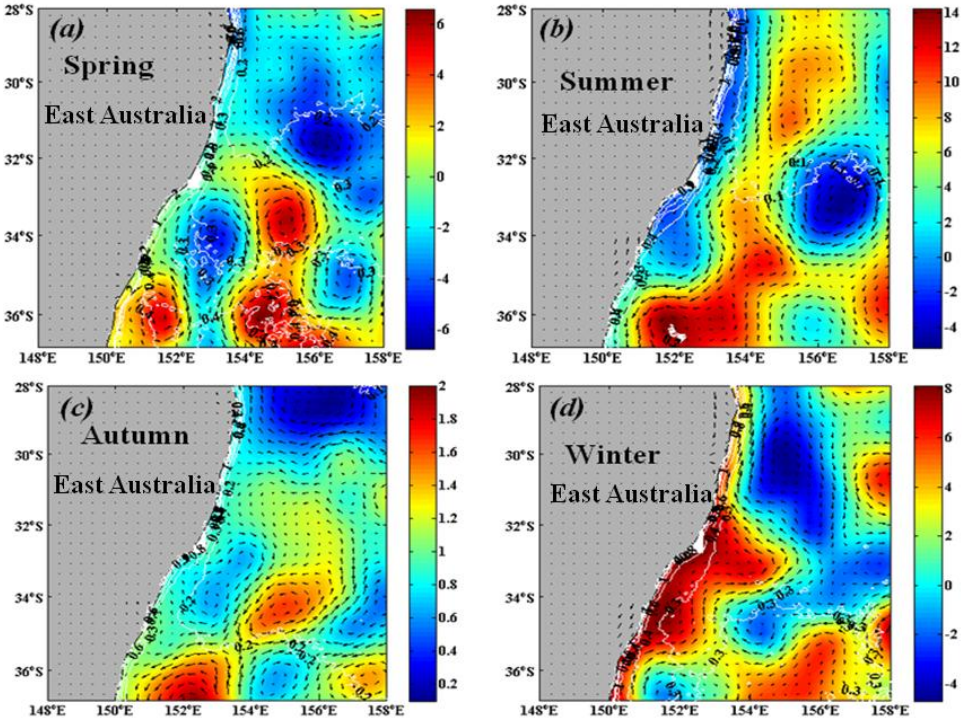

Figure 12: Geostrophic current (vectors) with SSHA (Sea Surface Height Anomaly) (shaded in m) during a) Austral Spring (September – November) b) Summer (December – February) c) Autumn (March-May) d) Winter (June – August) with white contours of Chl-a in mg m^{-3}.

3.7 Impact of Climate mode oscillations on Chlorophyll Variability in the EAC region

This section discusses how the Chl-a concentration varies across various phases of ENSO and SAM. ENSO is a two-to seven-year-periodic link between the atmosphere and the ocean that occurs in the Pacific Ocean. The interaction between the atmosphere and the ocean in the tropical Pacific results in a somewhat periodic variation between below-normal and above-normal SST and dry and wet conditions over the course of a few years.

To investigate the Chl-a variability during different ENSO phases, first, the ENSO phases were identified. El Niño is often referred to as the warm phase of ENSO, while La Niña is referred to as its cold phase. If the ENSO indices values are greater (lesser) than +1 (-1), then the phases for both climate events are positive (negative). The positive and negative phase of those indices is tabulated in Table 4.3 of chapter 4. A comparison of the composite Chl-a during El Niño and La Niña years was carried out, and the spatial variability of Chl-a concentration in relation to SST and MLD were analysed.

3.7.1 Comparison of Chlorophyll variation during El Niño and La Niña

The Chl-a concentration in the study area is always at its peak during the austral spring season (Fig. 11). Therefore, the Chl-a during austral spring was considered for the analysis different ENSO phases. La Niña composite shows the higher value of Chl-a on the south part of EAC region than that of El Niño composite (Fig. 13).

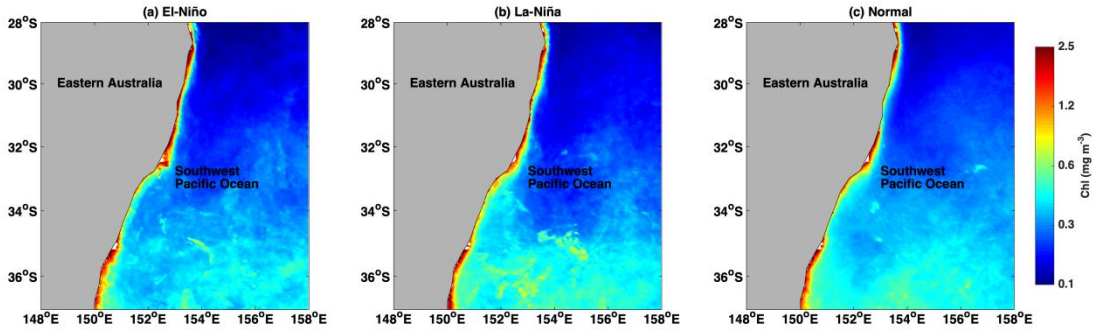

Figure 13: Area averaged Chl-a variability during the austral spring season (September-November) for a composite of (a) El Niño and (b) La Niña and (c) Normal years in the EAC region

During La Niña, an increase in Chl-a is detected not only in the shelf region but also in the southern region (south of 32°S) of the studied area. North of 32°S, no significant variation is seen (Fig. 13b). In the shelf region, the Chl-a is confined to the coast during El Niño. The Chl-a is extended more offshore from the shelf in La Niña, but the magnitude of the Chl-a is ~ 2.5 mg m^{-3} (in log10 scale) in both phases. In La Niña (El Niño), the Chl-a concentration increased (decreased) in the southern region is around 0.8 mg m^{-3} (0.4 mg m^{-3}) in log10 scale. To find out the reason behind this spatial variation in Chl, spatial variation of SST is considered as follows.

3.7.2 Chl-a variation during phases of SAM in the EAC region

The westerlies are moving away from Antarctica during the negative phase of SAM, and the impact can be seen in the study area. Higher wind speeds up the upper mixing of water, providing more nutrients to the phytoplankton. As a result, the negative phase of SAM has a higher Chl-a concentration (Fig. 14b). In the negative phase of SAM, Chl-a is more distributed on the shelf region (Fig. 14a), while in the positive phase, higher Chl-a is more restricted to the coast (Fig. 14b). The offshore of the study region's southern portion has a higher concentration of Chl-a of 1.25 mg m^{-3} than the counterpart of 2 mg m^{-3}. An account of the variation of SST during SAM is required to discuss this variation in Chl-a concentration.

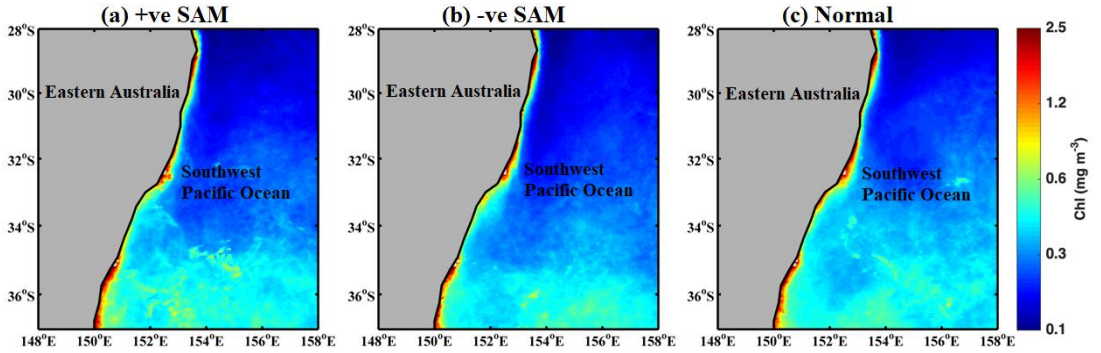

Figure 14: Area averaged spatial variation of Chl-a during the spring season (September-November) of (a) Positive SAM and (b) Negative SAM years in the EAC region

4. Conclusion

The aim of this study was to analyze the seasonal variability of Chl-a in the Atlantic and pacific ocean of the SO. The BMC in the Atlantic Ocean and EAC region in the Pacific Ocean was analyzed. The highest value of Chl-a was found to be 1.6 mg m^{-3} in the summer, and the lowest value was found to be 1.25 mg m^{-3} in the winter in the southwest Atlantic Ocean. The Chl-a in the BMC area is boosted by the nutrient-rich coastal water of the Brazil Current. Similarly, the stronger influence of the Malvinas current diminishes the Chl-a in this region. During the summer, Chl-a reached a peak of 1.6 mg m^{-3} (log10 scale) and then fell to 2.5 mg m^{-3} (log10 scale) during the winter. In this area, optimal PAR utilization (55 E m^{-2} d^{-1}) and frontogenesis mixing favors high Chl-a during the austral summer. SST, SSHA, and zonal wind stress all had a positive correlation with Chl, while meridional wind stress had a negative correlation. The concentration of Chl-a in the BMC area is modulated by ENSO and SAM as well. La Niña and the positive phases of SAM also show an increase in Chl-a concentration. In La Niña, the dominance of the nutrient rich Malvinas current favors the enhancement of Chl, whereas wind plays an important role in mixing and enhancement of Chl-a in the positive phase of SAM. The Rio de la Plata's river discharge also has a major impact on Chl-a concentration which was

evident from the fact that higher Chl-a concentrations were found at the river mouth followed by the BMC region.

During the summer, Chl-a levels near the coast reached a high of 2 mg m^{-3}, while during the winter, it fell to 0.4 mg m^{-3}. Coastal upwelling was more prevalent in the summer, resulting in higher Chl-a levels, while coastal downwelling is the primary cause of lower Chl-a levels in the winter. The EAC is strongest in the summer and gradually weakens in the winter. More dominant EAC means the lesser intrusion of Tasmania Sea water in this region. Frontal eddies resulted from the mixing of these two water masses, which is one of the reasons for Chl-a in the offshore area. Interannual variability of Chl-a was also prominent in the study region. A large annual variation is also observed in the southern extent of EAC. In the El Niño years and negative phase of SAM, the EAC extended up to ~34°S and in the La Niña and positive phase of SAM, the EAC extended up to ~32.5°S. This extent of EAC has more impact on the nutrient availability of the region. The strength of the EAC also varies annually. In La Niña, the strength of the EAC decreased and hence the influence of nutrient rich polar water increases, which leads to a higher Chl-a of 2.5 mg m^{-3} (in log10 scale) in the shelf region and 0.8 mg m^{-3} (in log10 scale). Due to the northward extension of westerlies, the southern part of the study region was affected by wind during the negative phase of SAM. This wind induced mixing in the southern portion of the southern ocean resulted in a 1.25 mg m^{-3} increase in Chl-a concentration.

References

[1] Acha, M., Mianzan, H., Guerrero, R., Carreto, J., Giberto, D., Montoya, N., Carignan, M., 2008. An overview of physical and ecological processes in the Rio de la Plata Estuary. Cont. Shelf Res. 28 (13), 1579—1588, http://dx.doi.org/10.1016/j.csr.2007.01.031.

[2] Artana, C., Ferrari, R., Koenig, Z., Saraceno, M., Piola, A. R., & Provost, C., 2016. Malvinas Current variability from Argo floats and satellite altimetry. Journal of Geophysical Research: Oceans, 121(7), 4854-4872.

[3] Campos, J.D., Lentini, C.A., Miller, J.L., Piola, A.R., 1999. Interannual variability of the Sea Surface Temperature in the South Brazilian Bight. Geophys. Res. Lett. 26 (14), 2061—2064, http://dx.doi.org/10.1029/1999GL900297.

[4] Ducet, N., Le Traon, P. Y., Reverdin, G., 2000. Global high-resolution mapping of ocean circulation from TOPEX/Poseidon and ERS-1 nd -2. Geophys. Research, 105:19,477-19,498. doi:10.1029/2000JC900063.

[5] Frenger, I., Gruber, N., Knutti, R., Münnich, M., 2013. Imprint of Southern Ocean eddies on winds, clouds and rainfall. Nature geoscience, 6(8): 608. doi: 10.1038/ngeo1863.

[6] Goni, G. J., & Wainer, I., 2001. Investigation of the Brazil Current front variability from altimeter data. Journal of Geophysical Research: Oceans, 106(C12), 31117-31128.

[7] Gordon, A. L., 1985. Indian-Atlantic Transfer of Thermocline Water at the Agulhas Retroflection. American Association for the Advancement of Science, 227(4690): 1030–1033. doi: 10.1126/science.227.4690.1030.

[8] Garzoli, S. L., & Giulivi, C., 1994. What forces the variability of the southwestern Atlantic boundary currents? Deep Sea Research Part I: Oceanographic Research Papers, 41(10), 1527-1550.

[9] Hassler, C.S., Djajadikarta, J., Doblin, M., Everett, J.D., Thompson, P.A., 2011. Characterisation of water masses and phytoplankton nutrient limitation in the East Australian Current separation zone during spring 2008. Deep Sea Research Part II: Topical Studies in Oceanography 58 (5), 664–677.

[10] George, J.V., Anilkumar, N., Nuncio, M., Soares, M.A., Naik, R.K., Tripathy, S.C., 2018. Upper layer diapycnal mixing and nutrient flux in the subtropical frontal region of the Indian sector of the Southern Ocean. Journal of Marine Systems, 187:197-205. doi: 10.1016/j.jmarsys.2018.07.007

[11] Huang, Z., and Feng, M., 2015. Remotely Sensed Spatial and Temporal Variability of the Leeuwin Current Using MODIS Data. Remote Sensing of Environment, 166: 214–232. doi:10.1016/j.rse.2015.05.028.

[12] Ji, C., Zhang, Y., Cheng, Q., Tsou, J., Jiang, T., & San Liang, X., 2018. Evaluating the impact of sea surface temperature (SST) on spatial distribution of chlorophyll-a concentration in the East China Sea. International journal of applied earth observation and geoinformation, 68, 252-261.

[13] Ji, C., Zhang, Y., Cheng, Q., Tsou, J., Jiang, T., & San Liang, X., 2018. Evaluating the impact of sea surface temperature (SST) on spatial distribution of chlorophyll-a concentration in the East China Sea. International journal of applied earth observation and geoinformation, 68, 252-261.

[14] Jullion, L., Heywood, K. J., Naveira Garabato, A. C., & Stevens, D. P., 2010. Circulation and water mass modification in the Brazil–Malvinas Confluence. Journal of Physical Oceanography, 40(5), 845-864.

[15] Kavak M T, Karadogan S., 2012. The relationship between sea surface temperature and chlorophyll concentration of phytoplanktons in the Black Sea using remote sensing techniques. Journal of Environmental Biology, 33 (2Suppl.): 493-498.

[16] Marshall, G.J., 2003. Trends in the Southern Annular Mode from observations and reanalyses. Journal of Climate, 16(24): 4134-4143. doi: 10.1175/1520-0442(2003)016<4134:TITSAM>2.0.CO;2

[17] Martinez, A., Ortega, L., 2015. Delimitation of domains in theexternal Río de la Plata estuary, involving phytoplanktonic and hydrographic variables. Braz. J. Oceanogr. 63 (3), 217—227, http://dx.doi.org/10.1590/S1679-87592015086106303.

[18] Nilsson, C., Cresswell, G., 1981. The formation and evolution of East Australian Current warm-core eddies. Progress in Oceanography 9 (3), 133–183.

[19] Oke, P.R., Middleton, J.H., 2000. Topographically induced upwelling off eastern Australia. Journal of Physical Oceanography 30 (3), 512–531.

[20] Richardson, P. L., Lutjeharms, J. R E, Boebel, O., 2003. Introduction to the 'Inter-Ocean Exchange

around Southern Africa. Deep-Sea Research Part II: Topical Studies in Oceanography 50 (1): 1–12. doi:10.1016/S0967-0645(02)00376-4.

[21] Ridgway, K.R., Godfrey, J., 1997. Seasonal cycle of the East Australian Current. Journal of Geophysical Research 102 (C10), 22921–22922.

[22] Roughan, M., & Middleton, J. H., 2002. A comparison of observed upwelling mechanisms off the east coast of Australia. Continental Shelf Research, 22(17), 2551-2572.

[23] Roughan, M., Oke, P. R., & Middleton, J. H., 2003. A modeling study of the climatological current field and the trajectories of upwelled particles in the East Australian Current. Journal of Physical Oceanography, 33(12), 2551-2564.

[24] Roughan, M., & Middleton, J. H., 2004. On the East Australian Current: variability, encroachment, and upwelling. Journal of Geophysical Research: Oceans, 109(C7).

[25] Rouault, M.J., Mouche, A., Collard, F., Johannessen, J.A., Chapron, B., 2010. Mapping the Agulhas Current from space: an assessment of ASAR surface current velocity. Journal of Geophysical Research, 115: 1-14. doi: 10.1029/2009JC006050.

[26] Simionato, C., Dragani, W., Meccia, V., Nuñez, M., 2004. A numerical study of the barotropic circulation of the Río de la Plata estuary: sensitivity to bathymetry, the Earth's rotation and low frequency wind variability. Estuar. Coast. Shelf Sci. 61 (2), 261—273, http:// dx.doi.org/10.1016/j.ecss.2004.05.005.

[27] Simionato, C., Vera, C., Siegismund, F., 2005. Surface wind variability on seasonal and interannual scales over Río de la Plata Area.84 L. Telesca et al./Oceanologia 60 (2018) 76-85 J. Coast. Res. 21 (4), 770783, http://dx.doi.org/10.2112/008-NIS.1.

[28] Telesca, L., Pierini, J.O., Lovallo, M. and Santamaría-del-Angel, E., 2018. Spatio-temporal variability in the Brazil-Malvinas Confluence Zone (BMCZ), based on spectroradiometric MODIS-AQUA chlorophyll-a observations. Oceanologia, 60(1), 76-85.

[29] Trenberth, K.E., Stepaniak, D.P., 2001. Indices of El Niño evolution. Journal of Climate, 14(8).1697-1701. doi: 10.1175/1520-0442(2001)014<1697:LIOENO>.2.0.CO;2

[30] Tilstone, G., Lotilker, A., Miller, P. I., Ashraf, P. M., Kumar T. S., Suresh, T., Ragavan, B. R. & Menon, H. B., 2013. Assessment of MODIS-Aqua chlorophyll-a algorithms in coastal and shelf waters of the eastern Arabian Sea. Continental Shelf Research, 65, 14-26. https://doi.org/10.1016/j.csr.2013.06.003